HOSTED BY
ELSEVIER
CrossMark
Available online at www.sciencedirect.com
ScienceDirect
Soils and Foundations 57 (2017) 341–356
SOILS AND FOUNDATIONS
www.elsevier.com/locate/sandf

Static liquefaction of very loose sand–slag–bentonite mixtures

Ayad Salih Sabbar, Amin Chegenizadeh *, Hamid Nikraz

Department of Civil Engineering, Curtin University, Perth, Australia

Received 18 April 2016; received in revised form 22 December 2016; accepted 25 January 2017
Available online 17 May 2017

Abstract

Static liquefaction is a highly destructive mechanism in the failure of soil deposits caused by a sudden loss of effective stress accompanied by vast deformations and a rapid build-up of pore water pressure that can cause soils to behave like liquids. This study examined liquefaction phenomena in saturated clean Perth sand, sand containing 3% bentonite, sand containing slag (2%, 4%, and 6%), and sand containing both 3% bentonite and slag (2%, 4%, and 6%). Undrained static triaxial compression tests were implemented on very loose mixtures at three initial confining pressures (100, 150, and 200 kPa). Static liquefaction (zero deviatoric stress and zero effective confining pressure) was observed at the lowest relative density and the lowest confining pressure. The liquefaction potential of the clean sand and the sand mixtures decreased with increases in confining pressure and relative density. The slag reduced the liquefaction susceptibility by reducing the inter-particle voids and producing a stable fabric. The optimum slag content was found to be 4%. Mixing clean sand with 3% bentonite produced a vulnerable fabric which exhibited high compressibility and a high level of excess pore water pressure. All sand–slag–bentonite mixtures showed non-flow behaviour and low excess pore water pressure. The mixture of sand with 4% slag and 3% bentonite exhibited the highest effective stress and the lowest excess pore pressure. It was revealed that the normalisation between the maximum and the minimum deviatoric stresses, namely, the brittleness index, can be used to quantify the liquefaction potential of clean sand and sand-slag-bentonite mixtures.

Keywords: Clean sand; Slag; Bentonite; Static liquefaction; Limited liquefaction; Non-flow behaviour; Brittleness index

1. Introduction

Liquefaction is one of the most complicated and debated topics in geotechnical engineering because it is used to define various contrasting, but related, phenomena (Kramer, 1996). Liquefaction has been widely studied, and researchers have devised a common definition for it. Liquefaction is a phenomenon involving a significant reduction in effective stress; it is accompanied by excessive strain and a build-up of pore water pressure when saturated soils are subjected to undrained static or cyclic loading (Castro, 1969; El Mohtar et al., 2013; Hird and Hassona, 1990; Jafarian et al., 2013; Kramer, 1996; NRC, 1985; Vaid and Sivathayalan, 2000; Verdugo and Ishihara, 1996; Yamamuro and Lade, 1997). The criteria for liquefaction failure can be divided into two main groups depending on the type of loading: flow liquefaction and cyclic mobility (Kramer, 1996; NRC, 1985). Flow liquefaction may occur when the static shear stresses applied to a soil are greater than the shear strength of the soil in its liquefied state (Kramer, 1996; NRC, 1985). Cyclic mobility may occur during cyclic loading; however, it is not considered here. Flow liquefaction produces the most devastating effects of all liquefaction types, and massive instabilities are termed 'flow failures' (Kramer, 1996; NRC, 1985). The flow failure mechanism requires a triggering method to initiate the liquefaction and undrained strain-softening (Sadrekarimi, 2014). Liquefaction flow failures have been

Peer review under responsibility of The Japanese Geotechnical Society.
* Corresponding author.
E-mail address: amin.chegenizadeh@curtin.edu.au (A. Chegenizadeh).

http://dx.doi.org/10.1016/j.sandf.2017.05.003
0038-0806/

investigated extensively by many researchers, and various analysis methods, procedures, and terminologies have been proposed (Kramer, 1996). Based on the results of previous studies, the response of cohesionless soils with different densities under monotonic undrained loading can be classified into three different types: liquefaction, limited liquefaction, and non-flow behaviour. Liquefaction is characterised by a rapid reduction in deviator stress that occurs after the peak point in the stress-strain curve and continues until reaching the criteria ($\sigma_3^- = 0$ or $\sigma_1 - \sigma_3 = 0$). In non-flow behaviour, the sand exhibits an increase in effective stress and a decrease in excess pore water pressure during shearing until the critical state. A limited flow response occurs in medium to loose sands when the strength of the sand decreases after the peak value in the stress-strain curve and is followed by increases in strength and decreases in pore water pressure at approximately large strains. Fig. 1 (a) and (b) shows the stress paths and stress-strain relationships, respectively, for the three types of behaviour under monotonic loading. The behaviour of liquefaction and limited liquefaction under static loading indicates a strain-softening type of undrained response (Vaid and Sivathayalan, 2000).

Different frameworks have been used to explain the behaviour of sandy soil under undrained static loading. Alarcon-Guzman et al. (1988) explained that the strain-softening of sandy soil depends on the concept of "structural collapse". According to this concept, cohesionless materials have unstable fabric in a loose state, and the contacts between the sand particles can be lost during undrained loading due to abrupt particle rearrangements. Eventually, the water undertakes the loads from the sand particles because of its relative incompressibility and inability to escape due to the speed of the phenomenon. The generation of excess pore water pressure depends on the changes in potential volume and the tendency to collapse. On the other hand, Been and Jefferies (2004) argued that the hypothesis for structural collapse is unable to explain the static liquefaction of sandy soil, as the flow failure response could be related to changes in the plastic strain rates rather than to sudden particle rearrangements. Andrade (2009) also observed that liquefaction phenomena are a function of the state of the sand rather than of the characteristics of the sand. Another framework connects the instability and the liquefaction of loose cohesionless soils under undrained static loading. Lade (1992) argued that instability is essential for liquefaction; however, they are not the same thing, even though both cause disastrous events. Fig. 1(a) shows the difference between a failure line and an instability line. Furthermore, Lade (1992) argued that the instability line indicates the beginning of the unstable states of stress. Instability can be demonstrated in the stress path $p^- - q$ curve. When there is a peak in deviatoric stress followed by a sudden decrease in effective stress, accompanied by the rapid build-up of pore water pressure, this instability produces large permanent deformations in soils which then flow towards failure (Andrade, 2009). Lade and Pradel (1990) and Pradel and Lade (1990) demonstrated that the unstable behaviour of granular materials is associated with their degree of saturation and with a switch from a drained to an undrained condition.

The relationship between the susceptibility of sandy soil to liquefy under undrained static loading and relative density and confining pressure has been investigated using different testing techniques, as summarized by Ibsen (1998), Kramer and Seed (1988) and Yamamuro and Lade (1997). The test results have shown that the susceptibility of sandy soil to undergo static liquefaction decreases with increases in relative density and confining pressure. Yamamuro and Lade (1997) showed that very loose sand samples exhibit anomalous behaviour under undrained static loading. This anomalous behaviour is characterised by increases in the shear strength of samples with an increasing confining pressure. However, the normal response should be that the strength of the samples decreases with an increasing confining pressure. Yamamuro and Lade (1997) explained that this unusual behaviour is due to the ability of the samples to compress, which leads to increases in relative density and, consequently, to the shear strength of the samples. Another relationship between the sample

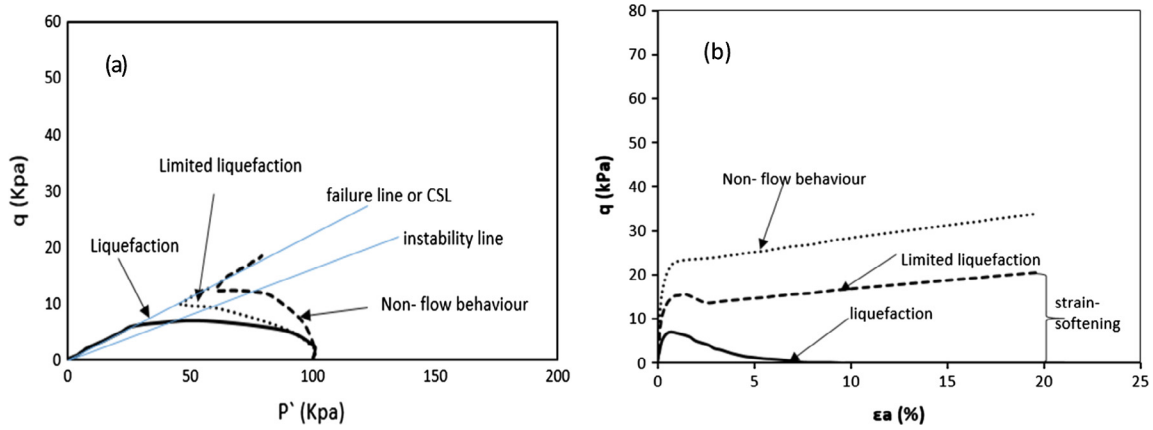

Fig. 1. Typical behaviour of sandy soil under undrained static loading.

preparation method and the liquefaction susceptibility of sandy soil was obtained by Miura and Toki (1982), Yamamuro et al. (2008) and Vaid and Sivathayalan (2000). The test results obtained from these studies showed further that samples prepared by the moist tamping method are more susceptible to liquefaction than samples prepared by other methods. Moist tamping produces a honeycomb fabric which is considered to be weak and creates substantial decreases in the void ratio during the saturation phase. Dafalias and Manzari (2004) defined the sand fabric as the normal orientation distribution of sand particles.

The influence of the fines particle content on the response of sandy soil under monotonic loading is an area of uncertainty due to the differing results obtained from previous studies. Some studies reported that the presence of the fines particle content reduces the ability of the sandy soil to liquefy (Seed et al., 1983; Pitman et al., 1994). In contrast, other studies concluded that the strength of sandy soil decreases with an increasing fines content, as its presence elevates soil compressibility by reducing the contacts between coarse particles (Rahman and Lo, 2014; Thevanayagam et al., 2002; Yand et al., 2006). There are also some studies which proposed a threshold around which the proportion of the fines content has a positive or negative effect. Belhouari et al. (2015) suggested that sandy soil shows a low tendency to liquefy when mixed with more than 30% silt. Yamamuro and Covert (2001) observed that sand with a high silt content (40%) exhibits more strain-softening behaviour than pure sand or sand with a low silt content. Yand and Wei (2012) examined the effects of two types of fines, namely, crushed silica and glass beads. Adding glass beads to sandy soil was found to reduce its ability to liquefy more than crushed silica. Pitman et al. (1994) noted that the behaviour of sandy soil shifts from limited liquefaction to a non-flow state as the sandy soil is mixed with increasing percentages (up to 40%) of crushed silica or kaolin. However, it was later shown by Georgiannou et al. (1990) that the liquefaction tendency increases with an increasing clay content. El Mohtar et al. (2013) observed higher pore water pressure in sand mixed with 3% and 5% bentonite than in clean sand, along with higher shear strength with an increasing curing time. Tang et al. (2013a) and Gratchev et al. (2006) reported that liquefaction susceptibility decreases as the bentonite content reaches >10% and ≥11%, respectively. Wei and Yang (2014) investigated the effect of the fines shapes on the static behaviour of sand–fine mixtures. They found that liquefaction susceptibility is more pronounced after adding rounded fines than after adding angular fines. Today, there is global interest in utilising slag for civil engineering applications due to the huge amount of slag that is produced and its problematic disposal. According to the Australian Slag Association (ASA, 2011), 3.4 million tonnes of iron and steel slag products were produced in Australia in 2009, some 80% of which was utilised in the construction of buildings and roads. Reusing this waste material has significant and positive environmental impacts involving resource conservation and reductions in carbon dioxide emissions. In geotechnical engineering, slag has been used extensively in the stabilisation of clay soils. However, it is difficult to find published research on the use of slag on its own for stabilising sandy soil. When slag makes contact with water, it reacts like Portland cement; however, it needs more time to achieve a full reaction, which is why it is sometimes mixed with a chemical activator. Ouf (2001) stated that the long reaction time of slag allows extra time for stabilisation work in the field. Matsuda et al. (2008) argued that granulated blast furnace slag could be used in geotechnical applications for liquefaction resistance because its shear strength increases with time. Additionally, they added that its geotechnical characteristics (high internal friction angle, light weight, and high permeability) make it useful for the backfilling of quay-wells, sand mats, and lightweight embankments. Several studies have reported that the shear strength of slag-stabilised sandy soil can be increased by using chemicals to activate the slag (Park et al., 2014; Rabbani et al., 2012; Yi et al., 2013).

A research program was recently started by the authors in collaboration with an investigation into the effects of the fines content on the liquefaction susceptibility of sandy soil. The aim is to examine the possibility of reducing catastrophic events caused by static liquefaction by using waste materials such as slag. It is apparent from the literature review that numerous investigations have been conducted on the effects of different fines contents. However, studies on the effects of mixing two types of fines on the static behaviour of sandy soil under undrained conditions are limited. Therefore, the aim of this study is to explore the responses of loose clean sand, and sand mixed with one percentage of bentonite and different percentages of slag, under static loadings, undrained conditions, and three different confining stresses. For this purpose, strain-controlled, undrained, static, and triaxial compression tests are conducted on isotropically consolidated samples of Perth sand containing 3% bentonite and various slag contents (2%, 4%, and 6% by weight), and sand mixed with two different fines.

2. Materials and testing method

2.1. Materials

Static compression triaxial tests were performed on soil specimens prepared by mixing Perth sand with 3% bentonite and 2%, 4%, and 6% slag by dry weight of sand, creating four binary and three triple mixtures. The sand used for the experiments was clean sand (99.98% sand and 0.2% silt), and the uniformity coefficient (C_u) and mean diameter (D_{50}) were equal at 2.235 and 0.35 mm, respectively. The sand was classified as poorly graded sand (SP) according to the Unified Soil Classification System (USCS). Grain size distribution curves for the sand and slag are

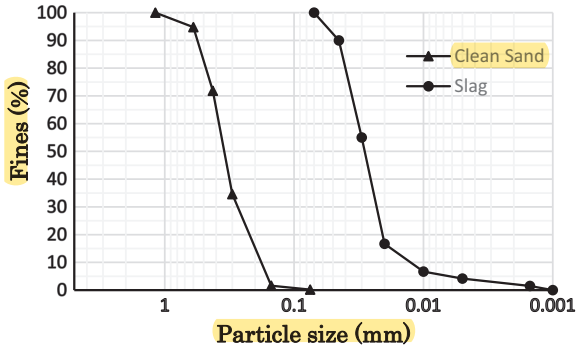

Fig. 2. Particle–size distribution curves for clean Perth sand and slag.

shown in Fig. 2. The bentonite used here was a sodium-based bentonite containing a high proportion of the active mineral species montmorillonite, manufactured by Unimin Australia Limited, Queensland, with at least 78% passing a 75 μm sieve and a bulk density of loose 1.0 (t/m^3). The chemical properties of bentonite are presented in Table 1. Slag can be defined as a by-product of iron and steel-making operations (Higgins, 2005). There are different types of slag based on the techniques used to produce iron. Blast furnace slag is a by-product of iron made in a blast furnace; it comes in three forms, namely, air-cooled, granulated, and expanded. Slag is widely used as an additive in structural engineering and, more recently, has also become a material of interest in geotechnical engineering (Allan and Kukacka, 1995; Yi et al., 2013). According to Veith (2000), there are environmental and economic considerations for using slag in soil stabilisation. Slag could be cheaper than other cementing agents due to the fact that it is a by-product and regarded as waste. The slag used in this study was granulated blast furnace slag (GBFS), manufactured by BGC Cement in Western Australia. It was coloured off-white, with a bulk density of loose of 1–1.1 tonne/m^3, a relative density of 2.85–2.95, and a surface area of 400–600 m^2/kg. The chemical properties are shown in Table 2. Scanning electron microscope (SEM) images of the sand, slag, and bentonite are presented in Fig. 3. The properties of the clean sand and the mixtures are shown in Table 3.

Bentonite and slag were added to the samples by dry-mixing them with oven-dried sand; their proportions were based on the dry weight of the sand before sample preparation. Triaxial tests were conducted on cylindrical specimens, 50 mm in diameter and 100 mm in height ($H/D = 2$), prepared by the moist tamping technique, which has been used in many previous studies (Bjerrum et al., 1961; Castro, 1969; Sladen et al., 1985; Kramer and Seed, 1988; Konrad, 1990; Ishihara, 1993; Pitman et al., 1994; Yamamuro and Lade, 1997). This method was chosen firstly to prevent segregation, and secondly to produce very loose samples (Murthy et al., 2007; Yand and Wei, 2012). In this study, very low relative densities (10% and 20%) were chosen to make the samples liquefy (Yamamuro and Lade, 1997). Experiments performed at high relative densities will be reported in a forthcoming publication. The method consisted of depositing a predetermined amount of soil into a circular split mould with a spoon and gently compacting it using a small tamper. Saturation of the samples was performed by simultaneously increasing the cell pressure and the pressure inside the specimen by keeping the effective confining pressure at 20 kPa throughout the saturation process. Applying back pressure from the bottom of the sample improved the sample saturation by compressing the air bubbles present between the sand particles (Delia, 2010). The samples were considered saturated when the B value reached 0.95. The back pressure applied to saturate the samples was varied with an increasing fines content. All samples were saturated in the range of 800–1000 kPa. All test specimens were isotropically consolidated under three different confining pressures (100, 150, and 200 kPa) before loading. Shearing was started as soon as possible after the consolidation stage to prevent the volumetric creep that occurs with time. All undrained compression triaxial tests for the current study were performed under strain-controlled circumstances at a constant strain rate of approximately 1 mm/min. This strain rate was enough to equalise the pore pressure inside the samples during the tests. All tests were continued until an axial strain of at least 20% was reached.

Table 1
Chemical component proportions of bentonite (mean % by weight).

Chemical component	%
Silicon dioxide (SiO_2)	63.6
Aluminium oxide (Al_2O_3)	14.6
Titanium dioxide (TiO_2)	0.4
Iron oxide (Fe_2O_3)	2.8
Calcium oxide (CaO)	0.3
Sodium oxide (Na_2O)	1.3
Magnesium oxide (MgO)	2
Potassium oxide (K_2O)	0.5
Loss on ignition	14.5

Table 2
Chemical component proportions of GBFS (mean % by weight).

Chemical component	%
Aluminium oxide (Al_2O_3)	5–15
Calcium oxide (CaO)	30–50
Silica, amorphous	35–40
Sulphur	<5

2.2. Testing method

A total of 27 undrained static triaxial tests were conducted on saturated loose specimens ($D_r = 10$ and 20%) under different testing conditions, such as three confining pressures (100, 150, 200 kPa). The testing program included eight types of samples produced by dry-mixing clean sand with different contents of bentonite and slag:

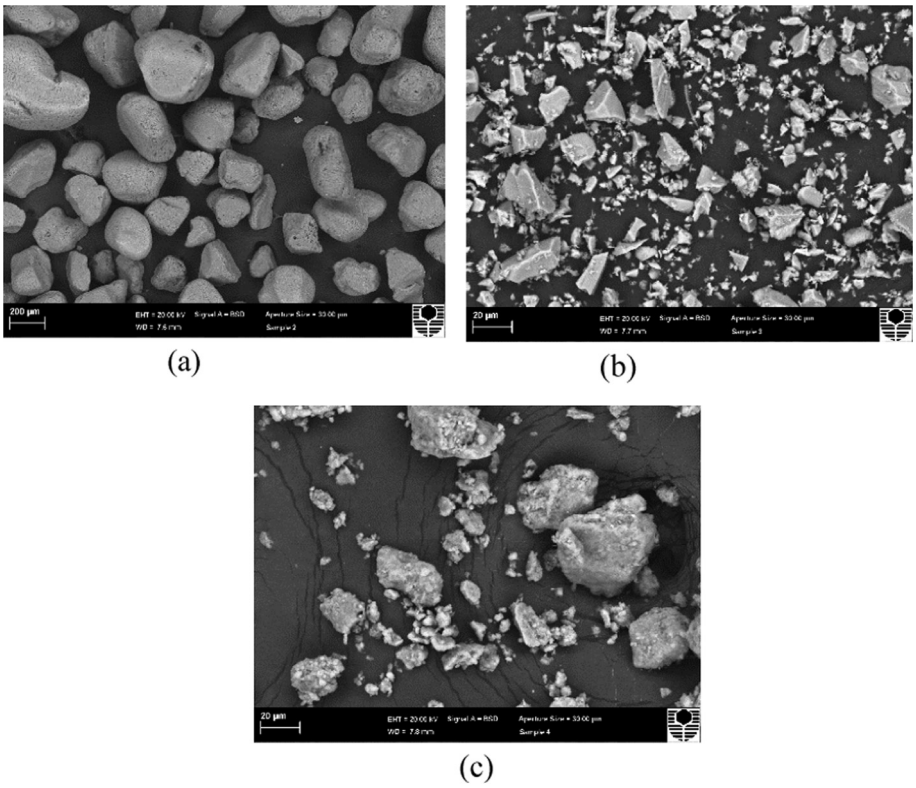

Fig. 3. Scanning electron microscope images of test materials: (a) clean sand; (b) GBFS slag; (c) bentonite.

Table 3
Physical properties of mixtures.

Materials	*GS*	e_{max}	e_{min}	e_o
Clean sand	2.580	0.675	0.544	0.6615
Sand + 2% Slag	2.613	0.649	0.548	0.6390
Sand + 4% Slag	2.630	0.646	0.546	0.6360
Sand + 6% Slag	2.640	0.644	0.544	0.6340
Sand + 3% Bentonite	2.614	0.657	0.492	0.6400
Sand + 2% Slag + 3% Bentonite	2.650	0.574	0.514	0.5680
Sand + 4% Slag + 3% Bentonite	2.680	0.565	0.497	0.5580
Sand + 6% Slag + 3% Bentonite	2.695	0.562	0.478	0.5535

Gs = specific gravity; e_{max} = maximum void ratio; e_{min} = minimum void ratio; e_o = initial void ratio.

clean sand (C.S), sand + 2% slag (S.2%S), sand + 4% slag (S.4%S), sand + 6% slag (S.6%S), sand + 3% bentonite (S.3%B), sand + 2% slag + 3% bentonite (Mix 1), sand + 4% slag + 3% bentonite (Mix 2), and sand + 6% slag + 3% bentonite (Mix 3). The tests are summarised in Table 4.

3. Results and discussion

3.1. Evaluation of undrained monotonic triaxial tests

Results of the undrained monotonic triaxial compression tests showed that the position of the maximum deviator stress of different effective stress paths – with different initial confining pressures with the same initial state – fell onto one line called the instability line (*IL*), which intersects the origin of the stress path. The *IL* can be used as a state boundary between the stable and the unstable behaviour of soil, in which all areas under the *IL* can be considered as the stable zone, while the areas above the *IL* can be considered the unstable zone (Jafarian et al., 2013; Leong et al., 2000; Yamamuro and Lade, 1997). Under undrained conditions, soil instability may occur in the area between the *IL* and the critical state line (*CSL*) (Yamamuro and Lade, 1997). The critical state can be defined as the state of the continuing deformation of the soil under constant stress and a constant void ratio (Murthy et al., 2007; Yamamuro and Lade, 1998). The *CSL* in the p^-–q stress path can be defined as the straight line which connects the origin and the points when the soil reaches the critical state. In the critical state soil concept, the relationship between deviatoric stress q and effective mean principal pressure p^- can be written as

$$q_{CSL} = M \times p^-_{CSL} \quad (1)$$

in which q_{CSL} and p^-_{CSL} are the deviatoric stress and the mean effective stress at the critical state, respectively, and M is the slope of the critical state line. According to Schofield and Wroth (1968), Eq. (1) can be written for the triaxial test cases as

$$\sin\phi_S = (3 \times M)/(6 + M) \quad (2)$$

where ϕ_S is the mobilised internal friction angle at the critical state.

Table 4
Summary of static triaxial tests performed (all samples isotropically consolidated).

No.	Materials	Symbol	D_{ri} (%)	P_o^- (kPa)	e_c	D_{rc} (%)	q_{max} (kPa)	U_{excess} (kPa)
1	Clean sand	C.S	10	100	0.6600	11.45	6.99	100
2	Clean sand	C.S	10	150	0.6560	14.50	11.84	140
3	Clean sand	C.S	10	200	0.6530	16.79	22.00	160
4	Clean sand	C.S	20	100	0.6475	20.99	15.6	50
5	Sand + 2% Slag	S.2%S	10	100	0.6373	11.58	12.59	58
6	Sand + 2% Slag	S.2%S	10	150	0.6338	15.05	13.11	98
7	Sand + 2% Slag	S.2%S	10	200	0.6290	19.80	21.7	108
8	Sand + 4% Slag	S.4%S	10	100	0.6349	11.10	16.59	44
9	Sand + 4% Slag	S.4%S	10	150	0.6325	13.50	16.65	80.5
10	Sand + 4% Slag	S.4%S	10	200	0.6275	18.50	26.91	99
11	Sand + 6% Slag	S.6%S	10	100	0.63268	11.32	11.23	74
12	Sand + 6% Slag	S.6%S	10	150	0.6293	14.70	10.93	100
13	Sand + 6% Slag	S.6%S	10	200	0.6225	21.5	21.96	121
14	Sand + 3% Bentonite	S.3%B	10	100	0.6370	12.12	5.61	95
15	Sand + 3% Bentonite	S.3%B	10	150	0.6300	16.36	7.12	141
16	Sand + 3% Bentonite	S.3%B	10	200	0.6236	20.24	9.77	187
17	Sand + 3% Bentonite + 2% Slag	Mix 1	10	100	0.5660	13.33	12.5	57
18	Sand + 3% Bentonite + 2% Slag	Mix 1	10	150	0.5650	15.00	22.99	42.75
19	Sand + 3% Bentonite + 2% Slag	Mix 1	10	200	0.5630	18.33	25.54	28
20	Sand + 3% Bentonite + 2% Slag	Mix 1	20	100	0.5610	21.67	45.00	40
21	Sand + 3% Bentonite + 4% Slag	Mix 2	10	100	0.5540	16.18	38.60	33
22	Sand + 3% Bentonite + 4% Slag	Mix 2	10	150	0.5520	19.12	31	51
23	Sand + 3% Bentonite + 4% Slag	Mix 2	10	200	0.5460	27.94	38	92
24	Sand + 3% Bentonite + 4% Slag	Mix 2	20	100	0.5487	23.97	58.00	20
25	Sand + 3% Bentonite + 6% Slag	Mix 3	10	100	0.5520	11.90	37.83	34
26	Sand + 3% Bentonite + 6% Slag	Mix 3	10	150	0.5480	16.67	24	70
27	Sand + 3% Bentonite + 6% Slag	Mix 3	10	200	0.5400	26.19	13.18	152

D_{ri} = initial relative density; P_o^- = initial confining pressure; e_c = void ratio after consolidation; D_{rc} = relative density after consolidation; q_{max} = peak deviator stress; U_{excess} = excess pore water pressure.

The shear strength of liquefied soil $S_{u(LIQ)}$ and yield strength $S_{u(yield)}$ has been used in several studies to determine the loss in undrained strength which could occur in sandy soil under undrained conditions. The peak undrained shear strength is represented by $S_{u(yield)}$, while the residual undrained shear strength is represented by $S_{u(LIQ)}$, as shown in Fig. 4. Many techniques are available for calculating $S_{u(yield)}$, the peak undrained shear strength of sandy soil, such as laboratory shear tests, numerical analyses such as constitutive models, and field penetration tests (Sadrekarimi, 2014). The $S_{u(yield)}$ value is profoundly dependent on mineralogy, gradation, structure, soil mixing effects, and sample disturbance. Several studies have suggested techniques for estimating the shear strength of liquefied soils (Poulos et al., 1985; Ishihara, 1993; Olson and Stark, 2003). These studies have defined the following procedures for calculating the $S_{u(yield)}$ and $S_{u(LIQ)}$ of liquefied soils:

$$S_{u(yield)} = q_{max}/2 \quad (3)$$

$$S_{u(LIQ)} = q_{min}/2 \times cos\ \phi_S \quad (4)$$

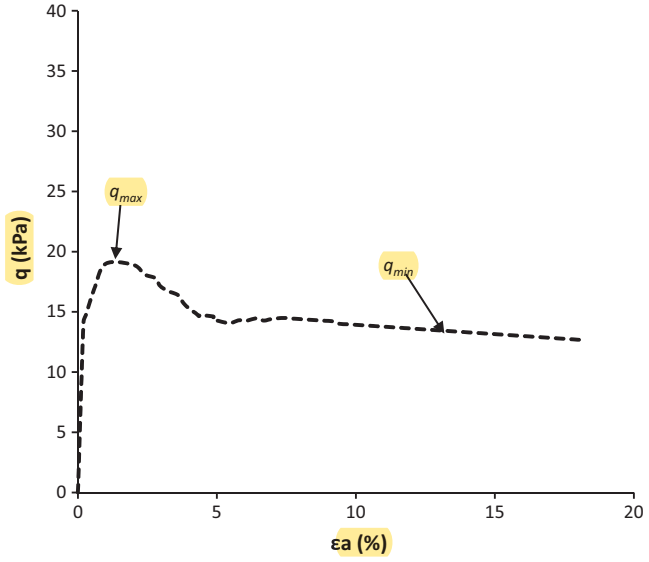

Fig. 4. Undrained static behaviour of saturated clean sand.

3.2. Behaviour of clean sand

3.2.1. Effect of confining pressure

Effective stress paths for undrained monotonic triaxial compression tests on saturated C.S samples with initial relative densities of about 10% are plotted on the Cambridge $p^- – q$ diagram, in which $p^- = (\sigma_1^- + 2\ \sigma_3^-)/3$ and $q = \sigma_1 – \sigma_3$, as shown in Fig. 5(b). As can be seen, all samples under the three different confining pressures showed strain-softening behaviour and generated positive excess pore water pressure (U_{excess}). In addition, the sample under the lowest

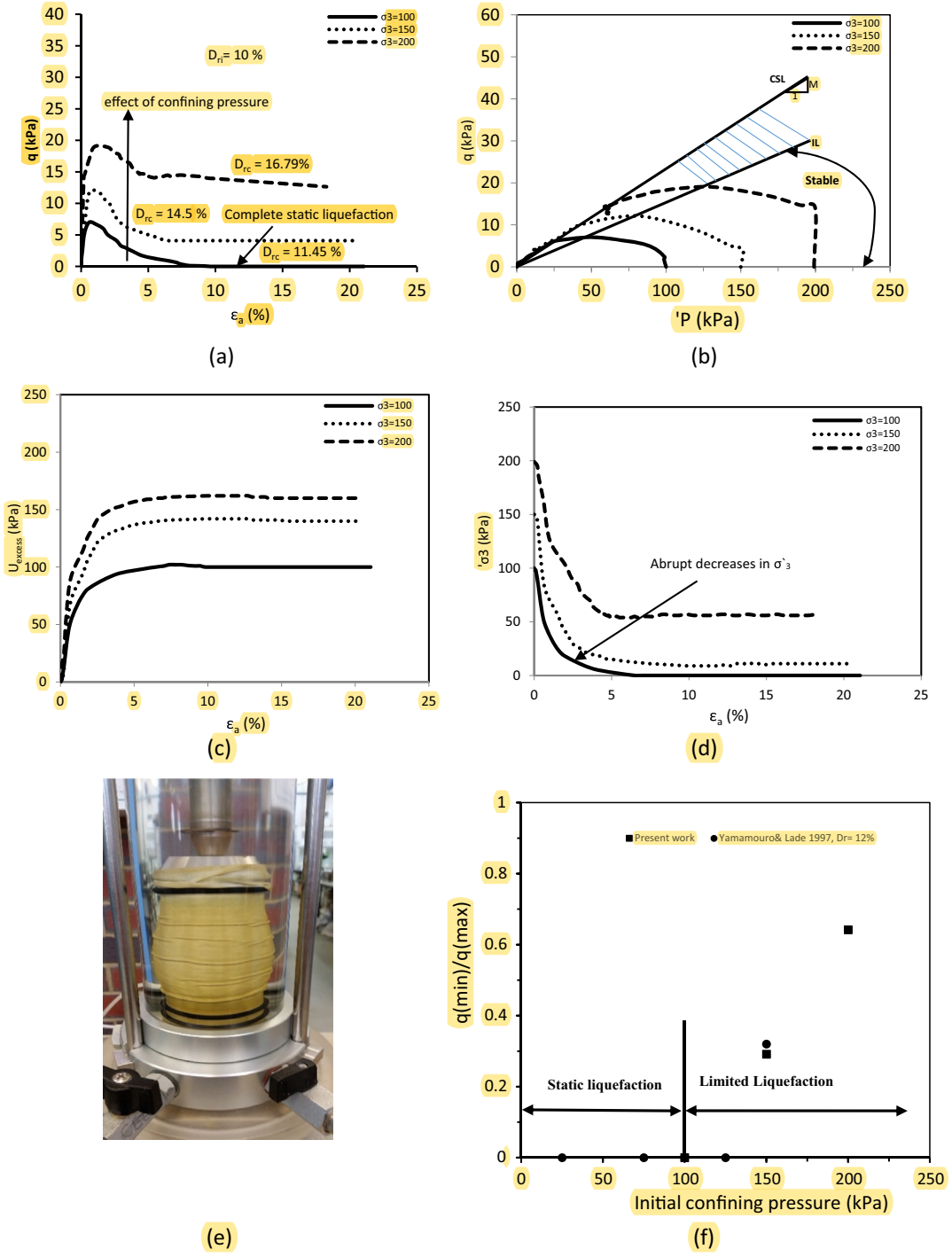

Fig. 5. Undrained static behaviour of saturated clean sand under different confining pressures: (a) stress–strain curves; (b) stress path; (c) excess pore water pressure–axial strain relation; (d) effective stress–axial strain relation; (e) wrinkles in membrane surrounding sample during static liquefaction; (f) q_{min}/q_{max} ratio–initial confining pressure relation.

initial confining pressure (100 kPa) exhibited complete static liquefaction as a result of the sudden increases in pore water pressure. When the pore water pressure reached the level of initial confining pressure, the effective stress was zero and the sample liquefied. The term "complete static liquefaction" can be described by

$$(\sigma_3^- = 0) \text{ and } (\sigma_1 - \sigma_3 = 0) \quad (5)$$

in which σ_1–σ_3 is the stress difference (deviator stress) and σ_3^- is the effective confining pressure.

These findings are consistent with past studies: the very loose sandy soil was liquefied under low confining pressures of 100 kPa or less (Ishihara, 1993; Riemer et al.,

1990; Yamamuro and Lade, 1997). Static liquefaction was accompanied by the generation of large wrinkles in the membrane surrounding the specimens (Fig. 5(e)); this is indicative of the uniform pattern of internal deformations (Lade, 1992; Yamamuro and Lade, 1997). Fig. 5(b) shows that the peak deviatoric stress of the samples increased with an increasing confining pressure (Fig. 5(a)) which represents the stress–strain relations. Fig. 5(a) reveals that the samples under initial confining pressures of 150 and 200 kPa showed greater deviatoric stress than the samples under an initial confining pressure of 100 kPa. After the peak value, the excess pore water pressure reached a value lower than the initial confining pressures, and samples exhibited constant strength as the stress difference did not reach zero. Moreover, the greater the confining pressure was, the more rapidly the pore water pressure was generated (Fig. 5(b) and (c)). Fig. 5(d) indicates that the effective confining pressure rapidly dropped from an initial value at the commencement of shear. Testing at the initial confining pressure of 100 kPa approached the minimum values ($\sigma_3^- = 0$) at 6.5% axial strain due to the tendency of very loose cohesionless materials to compress, which reduced the effective stress and increased the excess pore water pressure. However, samples under confining pressures of 150 and 200 kPa approached the minimum values ($\sigma_3^- \neq 0$) at 8% and 10% axial strains, respectively. This is related to increases in effective stress and decreases in excess pore water pressure after increases in initial confining pressure. The effect of the confining pressure on the liquefaction susceptibility can also be observed by drawing the relationship between the ratio of minimum deviator stress to the peak deviator stress (q_{min}/q_{max}) and initial confining pressure. As shown in Fig. 5(f), this relationship could be used to show the confining pressure at which liquefaction takes place. A q_{min}/q_{max} ratio of 0.0 represents complete static liquefaction and a ratio of 1.0 accounts for a non-flow response. Fig. 5(f) shows that the ratio of q_{min}/q_{max} was zero at an initial confining pressure of 100 kPa, indicating complete static liquefaction. The ratio then increased at initial confining pressures of 150 and 200 kPa, indicating that the specimens exhibited stable behaviour with less liquefaction susceptibility. Also, Fig. 5(f) shows insignificant differences between the deviator stress ratio and the initial confining pressure in the present study. This is compared with Yamamuro and Lade's (1997) study conducted on very loose Nevada sand ($D_r = 12\%$) at various initial confining pressures of 25–150 kPa. The effect of the initial confining pressure on the behaviour of very loose C.S samples can be considered as anomalous behaviour. The word *anomalous* is used here to describe the behaviour of very loose samples when the shear strength increases with an increasing confining pressure. In contrast, normal behaviour is when the strength of the samples decreases with an increasing confining pressure, which has been reported in many previous studies (e.g., Alarcon-Guzman et al., 1988; Vaid and Chern, 1985). According to Yamamuro and Lade (1997) and Yamamuro and Covert (2001), the main reasons for the "reverse" behaviour of C.S are related to the densification of the samples during their consolidation, brought about by rapid decreases in sample compressibility with an increasing initial confining pressure. The reduction in compressibility indicates better contacts between sand particles which then produces high soil fabric stiffness. Consequently, the excess pore water pressure decreases. The effect of densification during consolidation can be noticed when the initial relative density of the samples increases from 10 to 11.45, 14.5, and 16.79% at confining pressures of 100, 150, and 200 kPa, respectively, as shown in Fig. 5(a), in which D_{rc} is the relative density after consolidation.

3.2.2. Effect of relative density

The influence of increases in the relative density of very loose C.S was examined by conducting undrained tests on clean Perth sand with initial relative densities of 10% and 20%, an initial confining pressure of 100 kPa, and fully saturated samples ($B = 0.95$). The relationships of stress vs. strain, stress paths, effective confining pressures vs. axial strain, and excess pore water pressure vs. axial strain are shown in Fig. 6(a)–(d), respectively. Fig. 6(b) shows that the initial slope of the effective stress path of C.S increased as the relative density increased from 10% to 20% due to a reduction in pore water pressure, which indicates that liquefaction susceptibility declines with an increasing relative density. This relationship can be clearly seen in Fig. 6(a), when the behaviour of soil transforms from complete static liquefaction at $D_{ri} = 10\%$ to limited liquefaction at $D_{ri} = 20\%$. Yamamuro and Lade (1997) showed that Nevada sand completely liquefied at a very low relative density of 12%, while samples exhibited limited liquefaction and completely stable behaviour after increasing relative densities to 31% and 42%, respectively. Fig. 6(c) and (d) shows that at 10% relative density, the effective confining stress was dramatically reduced (indicating complete static liquefaction) under sudden increases in excess pore water pressure, until it matched the initial confining pressure (100 kPa) at very low axial stress. However, at a relative density of 20%, the effective confining stress gradually decreased with slow increases in excess pore water pressure, and then increased as the excess pore water pressure decreased at an axial strain of 5%, indicating limited liquefaction. The improvement of the shear strength of the samples with an increasing relative density could be connected to the stability of the sand fabric, which improved due to the increases in inter-particle contacts and to the decreases in sample compressibility. The stable sand fabric reduced the rate of the pore water pressure and increased the effective stress, finally producing more stable behaviour. The positive effect of relative density on the static liquefaction resistance of sandy soil has been broadly observed by numerous researchers. Many studies have pointed out that sandy soil shifts from liquefaction behaviour to stable behaviour with increases in relative density, initial confining pressure, and shear parameters.

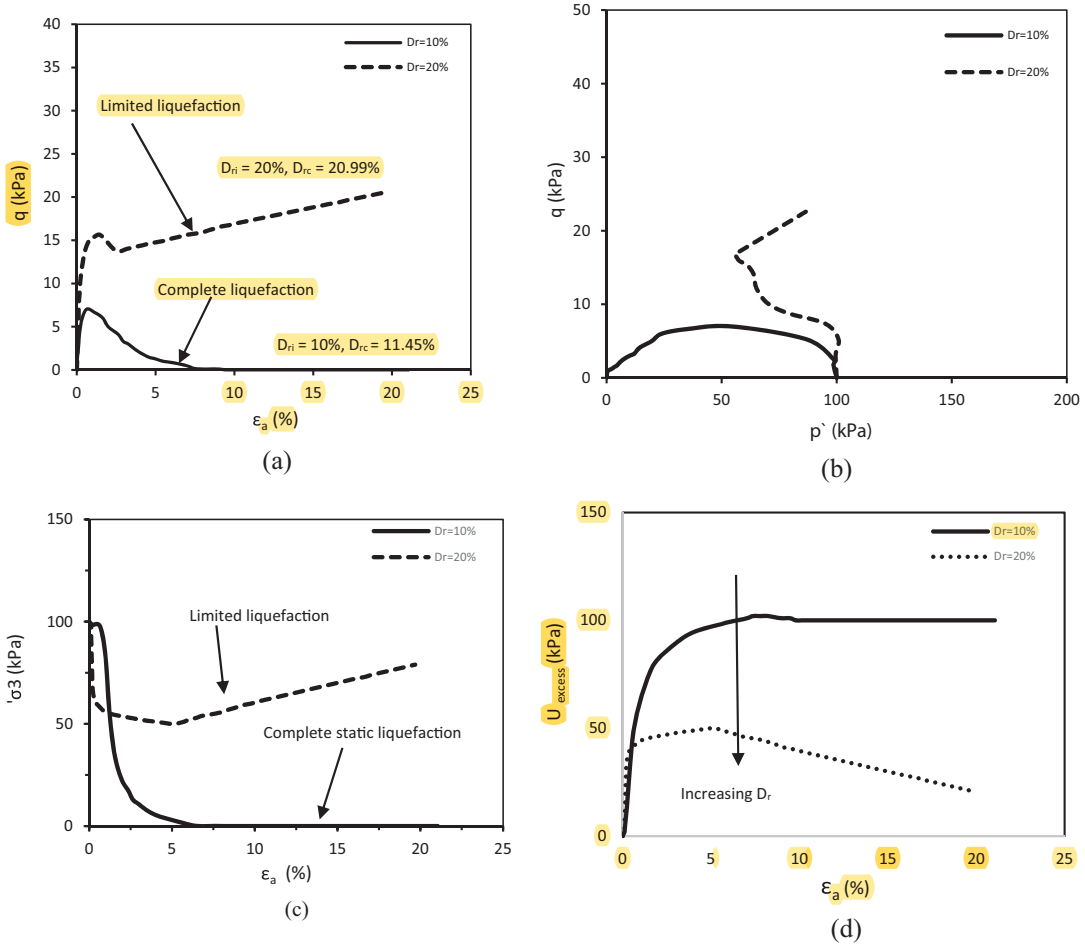

Fig. 6. Undrained static behaviour of saturated clean sand under different relative densities: (a) stress–strain curves; (b) stress path; (c) effective stress–axial strain relation; (d) excess pore water pressure–axial strain relation.

3.3. Effect of slag on static behaviour of sandy soil

A series of undrained isotropically-monotonic triaxial tests were conducted on sand–slag mixtures to evaluate the effect of the slag content on the behaviour of the treated sandy soil. The clean Perth sand was mixed with three different slag contents (2%, 4%, and 6%) based on the dry weight of the sand. Samples were tested under $D_{ri} = 10\%$, $B = 0.95$, 0–day curing time, and three initial confining pressures of 100, 150, and 200 kPa. Figs. 7 and 8 show that complete static liquefaction ($\bar{\sigma_3} = 0$) occurred in the C.S samples with the lowest initial confining pressure (100 kPa), while none of the three mixtures (S.2%S, S.4% S, and S.6%S) liquefied at the same confining pressure, indicating that their behaviour changed from unstable to stable with an increasing slag content. This is shown by examining q–ε_a in Fig. 7. The stress–strain curves of the mixtures show that the deviatoric stress did not reach zero, as in the test indicating complete static liquefaction, but decreased and then increased to the level well above the initial peak, indicating the condition of limited liquefaction. The deviatoric stresses of all the samples – C.S, S.2%S, S.4%S, and S.6%S – increased with an increasing confining pressure, and the S.4%S mixture showed the greatest deviatoric stresses under initial confining pressures of 100, 150, and 200 kPa. The effect of the slag content on the behaviour of the C.S samples can be observed in Fig. 9(d), which shows that stress ratio q_{min}/q_{max} increased when the slag content was increased from 2% to 4%, and decreased with the 6% slag content. Moreover, it shows that the stress ratio increased with an increasing confining pressure and that the stress ratio values were between 0 and 1, which indicates limited liquefaction behaviour. This behaviour is related to the effect of fines when they comprise more than 4% of the mixture, which is to increase the compressibility of the samples and, consequently, to reduce the liquefaction resistance by increasing the excess pore water pressure and decreasing the effective confining pressure. Fig. 9 shows that the excess pore water pressures generated in the sand–slag mixtures were less than the pore water pressure in C.S. Excess pore water pressure U_{excess} was reduced from 100 kPa to 31, 14, and −46 kPa at slag contents of 6%, 2%, and 4%, respectively, at a confining pressure of 100 kPa. At a confining pressure of 100 kPa, there was an abrupt increase in the rate of pore water pressure in C.S, whereas the pore water pressure increased

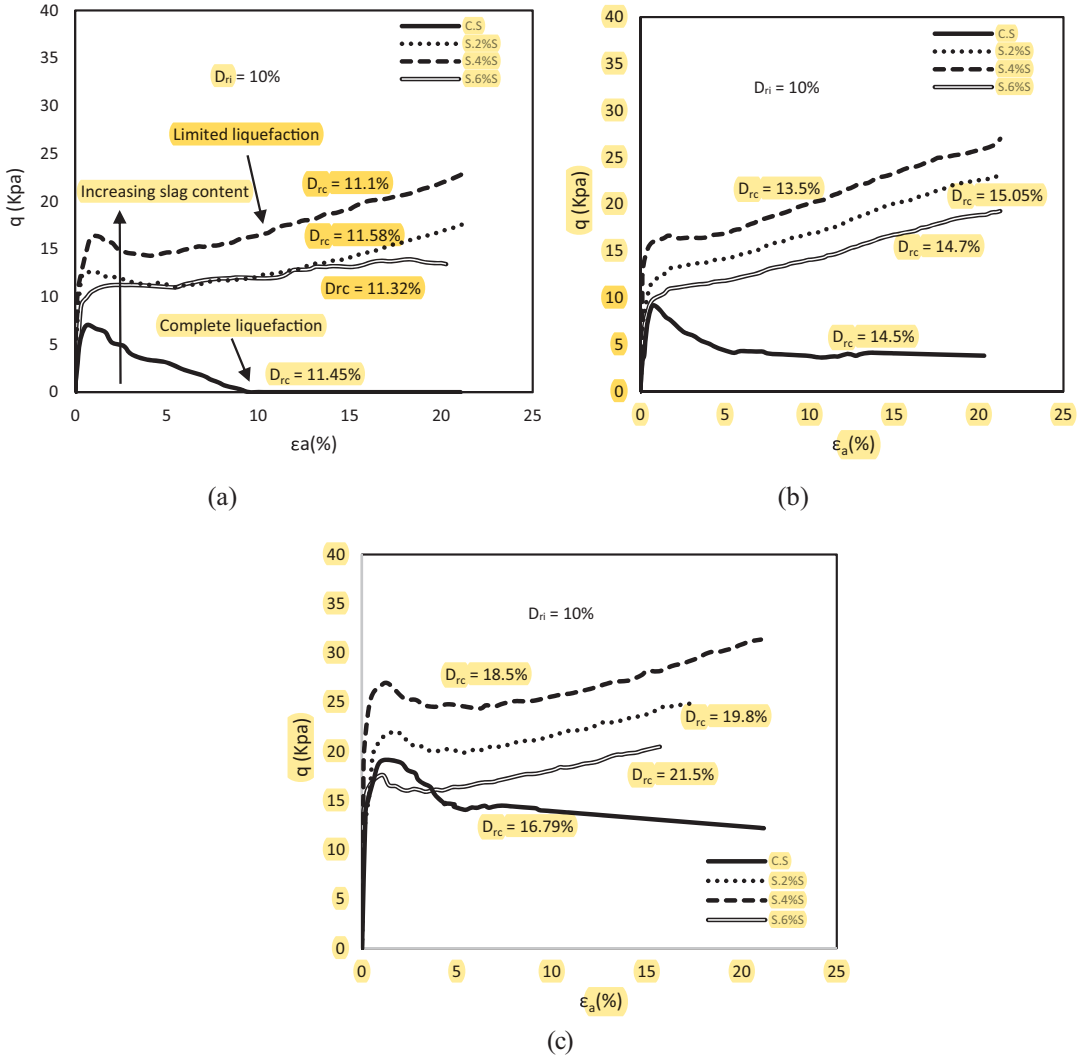

Fig. 7. Undrained static behaviour of clean sand mixed with different slag contents with $D_r = 10\%$ and $B = 0.95$: (a) stress–strain curves with $\sigma_3 = 100$ kPa; (b) stress–strain curves with $\sigma_3 = 150$ kPa; (c) stress–strain curves with $\sigma_3 = 200$ kPa.

gradually in the sand–slag mixtures, and the S.4%S mixture showed the lowest pore water pressure at the same confining pressure. The negative value for the excess pore water pressure indicates non-flow behaviour in the samples. The positive impact of the slag content on the behaviour of sandy soil could be related to mechanical, rather than chemical, effects. The slag may react as a chemical additive and increase the strength of the soil when it is fully hydrated and cured. However, in this study, the tests were conducted without considering the slag curing time due to the complexity of the effect; it can be considered as future work. Therefore, the liquefaction susceptibility of sandy soil decreased with the fines content due to the role of slag as a fines additive which filled the voids between the sand particles and increased the contacts between the sand grains. Hence, the slag reduced the pore water pressure and stabilised the sample fabric. Previous studies on the effect of slag on the behaviour of sandy soil are rare; and hence, comparisons cannot be made. Almost all previous studies focused on using slag to improve the mechanical properties of soft clays and expansive soils. All of them indicated that slag improved the shear strength of soft clay soils and reduced the expansion of expansive soils.

3.4. Effect of bentonite on static behaviour of clean sand

A series of undrained isotropically-consolidated monotonic triaxial tests was conducted to characterise the behaviour of sand–bentonite mixtures under static loading. The tests were run on saturated, very loose samples ($D_{ri} = 10\%$) with 3% bentonite at three different confining pressures of 100, 150, and 200 kPa. Fig. 10 shows that the presence of 3% bentonite did not improve the shear strength of the sandy soil. This behaviour is demonstrated in Fig. 10(a) where the deviatoric stress of the S.3%B samples was less than the deviator stress of C.S under the three confining pressures. Additionally, the increase in the deviatoric stresses of the S.3%B samples was less than for the C.S samples

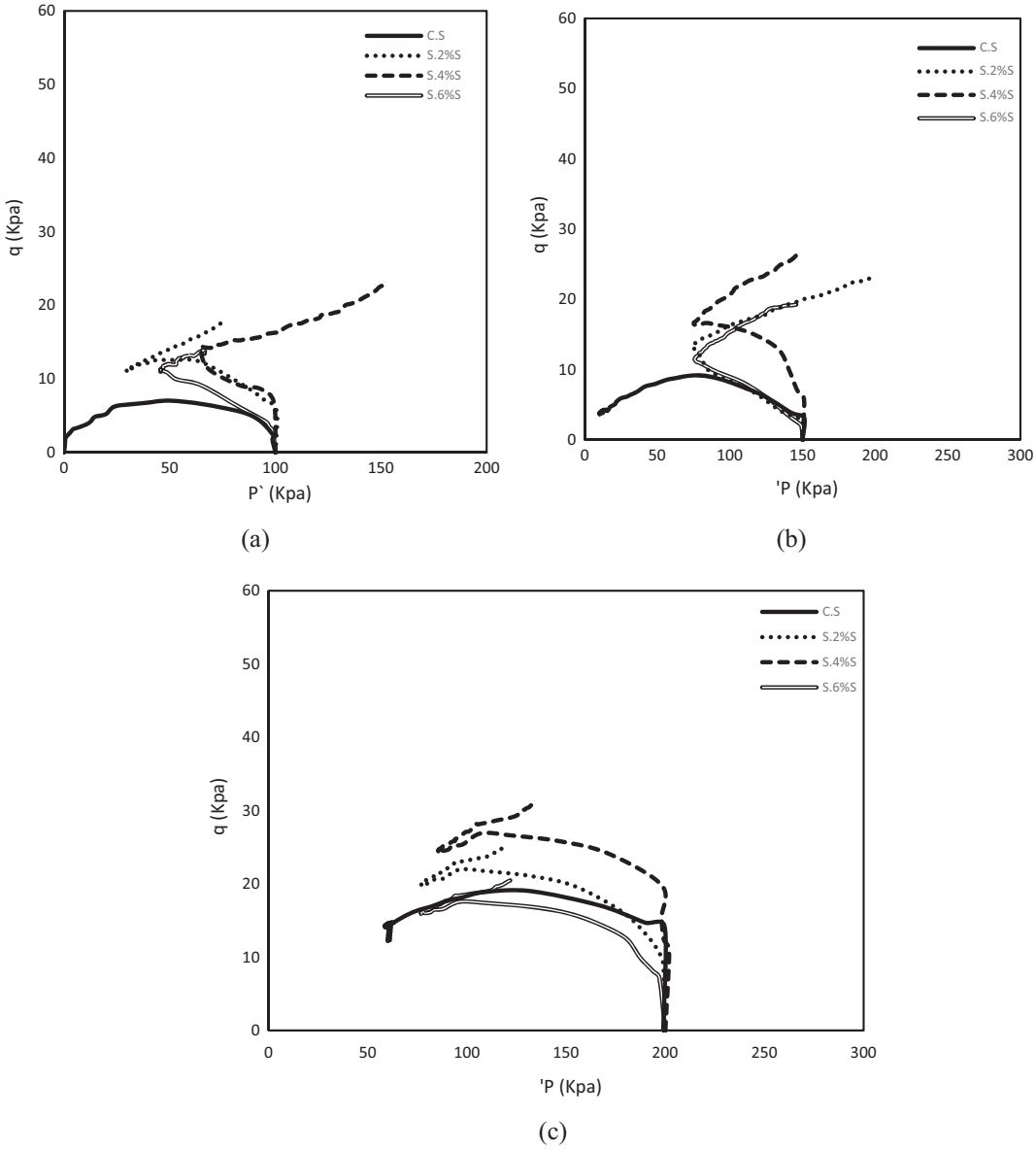

Fig. 8. Undrained static behaviour of clean sand mixed with different slag contents with $D_r = 10\%$ and $B = 0.95$: (a) stress path with $\sigma_3 = 100$ kPa; (b) stress path with $\sigma_3 = 150$ kPa; (c) stress path with $\sigma_3 = 200$ kPa.

with an increasing confining pressure. Fig. 10(c) indicates a tendency for increases in compression for the S.3%B specimens when the effective confining pressure significantly decreases, meaning abrupt increases in the generation of excess pore pressure eventually enhanced the potential for static liquefaction. The rate of generation of excess pore pressure in S.3%B was higher than in C.S: U_{excess} was 187 kPa at a confining pressure of 200 kPa for S.3%B, while it was 147 kPa in C.S at the same confining pressure. The negative impacts of bentonite on the behaviour of sandy soil would be related to the production of an unstable fabric, as a low bentonite content causes sand grains to be slippery and increases compressibility. This finding is consistent with the past studies of Tang et al. (2013a,b) and El Mohtar et al. (2013), who reported that the liquefaction potential increased with bentonite contents of <5%. However, Gratchev et al. (2006) noted that artificial clay-sand mixtures exhibited rapid liquefaction when the bentonite content was ≤7%, while liquefaction susceptibility was reduced with bentonite contents ≥11%. The effect of the curing time on the sand–bentonite mixtures was not explored in this study as it has already been extensively investigated in the literature. These studies reported that the undrained shear strength of sand–bentonite mixtures increases and that the generation of excess pore pressure decreases with increasing curing periods. The study by El Mohtar et al. (2013) also found that the generation of excess pore pressure in sand mixed with 3% and 5% bentonite decreased with an increasing curing age.

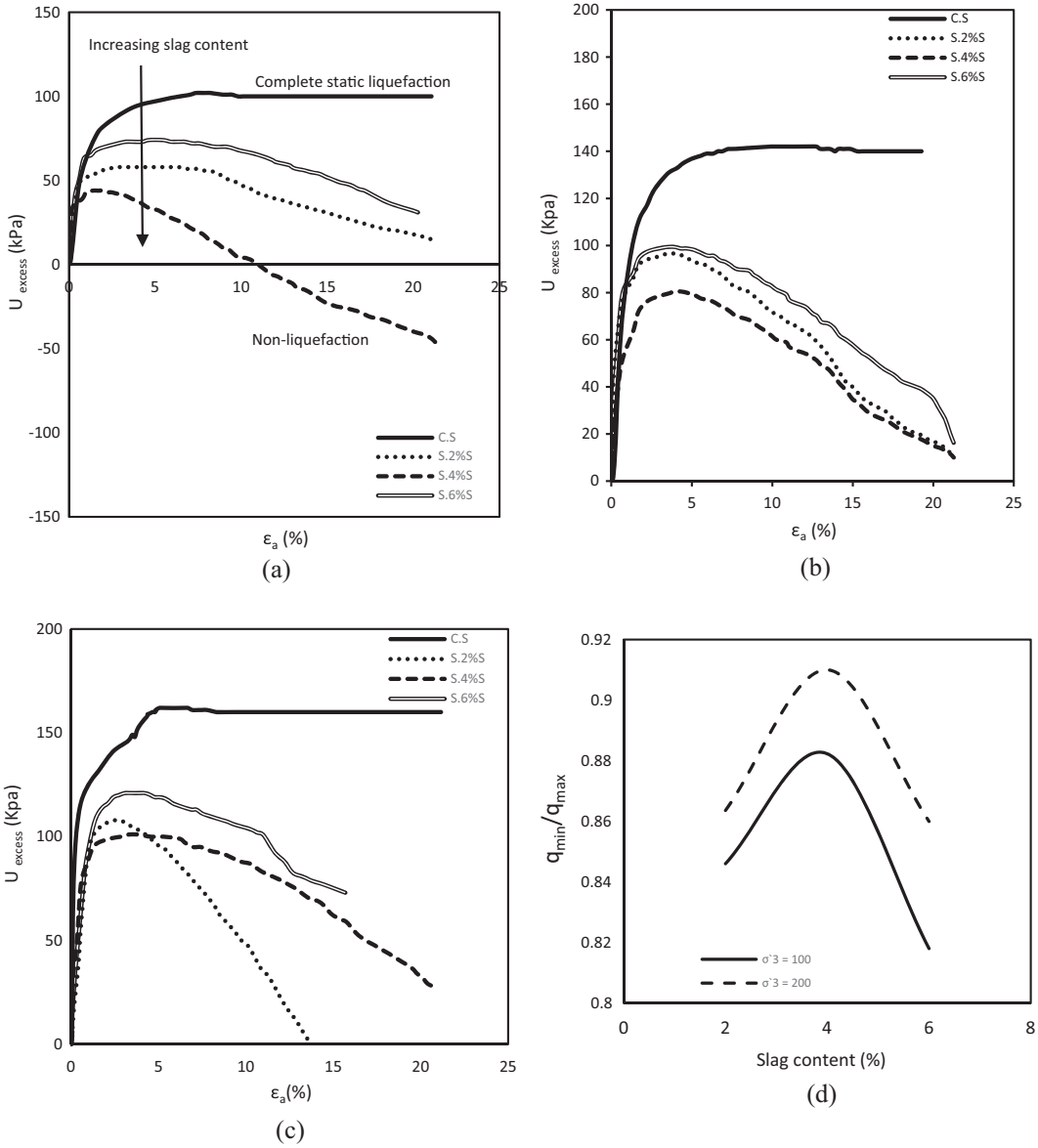

Fig. 9. Undrained static behaviour of clean sand mixed with different slag contents with $D_r = 10\%$ and $B = 0.95$: (a) excess pore water pressure – axial strain with $\sigma_3 = 100$ kPa; (b) excess pore water pressure – axial strain with $\sigma_3 = 150$ kPa; (c) excess pore water pressure – axial strain with $\sigma_3 = 200$ kPa; (d) slag content – stress ratio.

3.5. Behaviour of sand-slag-bentonite mixtures

The effect of a combination of two different fines on the behaviour of sandy soil under static loading is shown in Fig. 11. A series of undrained static triaxial tests with $D_{ri} = 10\%$, $B = 0.95$, and confining pressures of 100, 150, and 200 kPa was performed on three different mixtures, called Mix 1, Mix 2, and Mix 3. The data from undrained tests demonstrated that the three blends exhibited non-flow behaviour, while the C.S samples exhibited complete static liquefaction responses at the same confining pressures. This data indicates that the liquefaction susceptibility of the three mixtures was lower than for C.S, and that no single combination showed complete static liquefaction under the three confining pressures. The non-flow behaviour can be observed by examining the effective confining pressure and excess pore pressure curves. Fig. 11(c) shows that the effective confining pressure in C.S dramatically decreased at slight axial strain; however, Mix 1, Mix 2, and Mix 3 showed gradual reductions followed by increases in effective confining pressures. Fig. 11(d) illustrates that the rate of excess pore pressure generation in the mixtures was lower than for C.S, due to the potential improvement in the sand fabric when mixed with two different fines. Mix 2 (4% slag, 3% bentonite) showed the highest values of deviatoric stress, while Mix 3 (6% slag, 3% bentonite) showed the lowest values. In addition, Mix 2 showed deviatoric stresses that were greater than those of the slag and the bentonite separately. All samples of C.S and the three mixtures showed increasing deviatoric

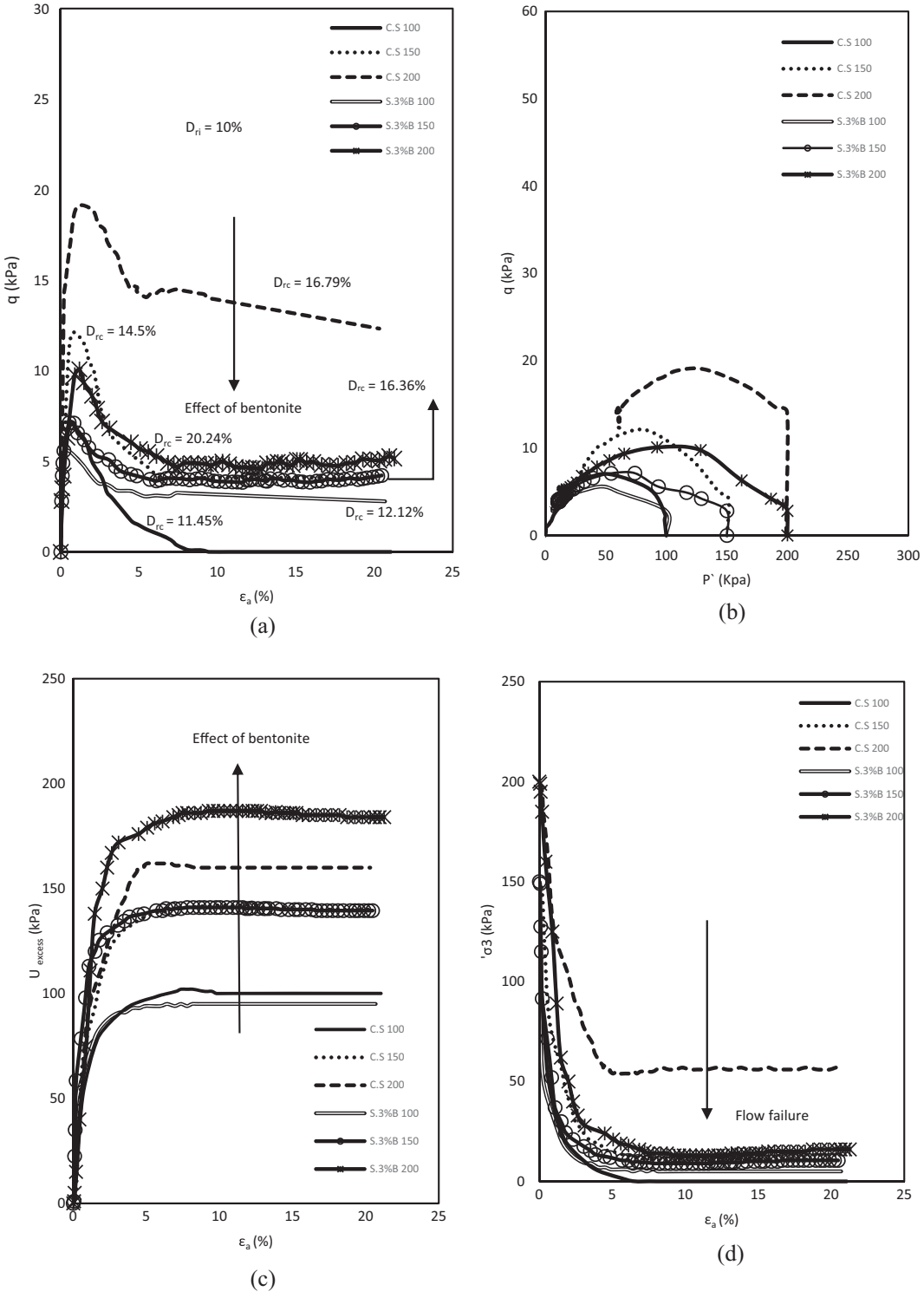

Fig. 10. Undrained static behaviour of saturated clean sand mixed with 3% bentonite with $D_r = 10\%$: (a) stress–strain relation; (b) stress path; (c) excess pore water pressure – axial strain relation; (d) effective confining pressure – axial strain relation.

stresses with increases in initial confining pressure. The results of undrained tests under confining pressures of 150 and 200 kPa are not presented in this section. The roles of slag and bentonite in the strength enhancement of samples were noticeable when their behaviour shifted from complete static liquefaction and limited liquefaction in pure or single-additive samples (clean sand, sand mixed with slag only, and sand mixed with bentonite only) to non-flow behaviour when sand was mixed with both additives. This effect could be connected to the function of fines in improving the sand fabric by increasing the particle connections. Moreover, the chemical components of slag and

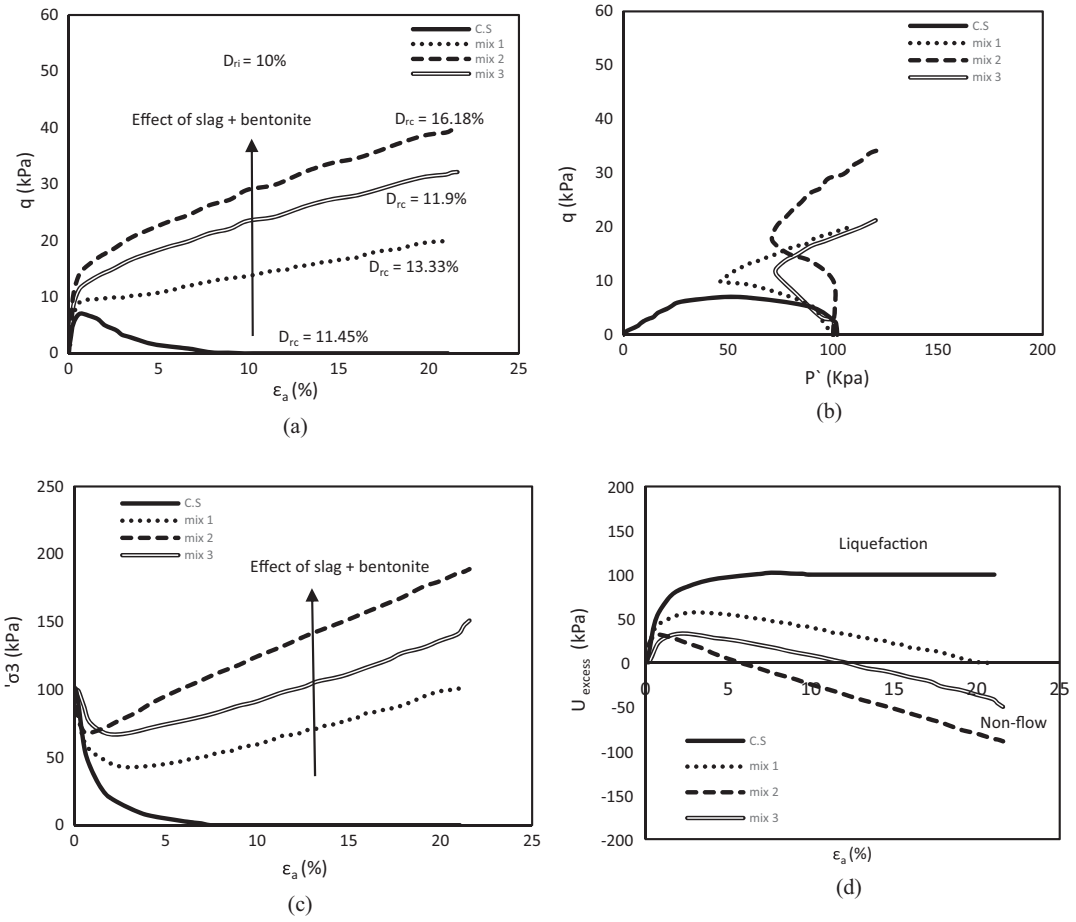

Fig. 11. Static undrained behaviour of Mix 1, Mix 2, and Mix 3 with $D_r = 10\%$ and $B = 0.95$: (a) stress–strain relation; (b) stress path; (c) excess pore pressure–axial strain relation; (d) effective confining pressure – axial strain.

bentonite may play significant roles in reducing the liquefaction potential of mixtures. These findings are consistent with previous studies, which have shown that fines have a significant effect on the static behaviour of sandy soil.

3.6. Effect of liquefaction

Values q_{max} and q_{min} are used in this study to measure the magnitudes of the decline in undrained shear strength that occurs following the initiation of static liquefaction. The amount of shear strength loss beyond liquefaction has a significant effect on its consequences (Kramer and Seed, 1988). During liquefaction, the soil element achieved q_{max} at very low strain and then q_{max} dropped until it reached minimum deviatoric stress (q_{min}). Some of the undrained triaxial static tests showed an increase in deviatoric stress towards the end of the test after a reduction in the peak deviatoric stress. In this case, the minimum values of deviatoric stress (occurring after its drop but before its increase) are denoted as q_{min} (Ishihara, 1993; Yoshimine et al., 1999). Flow failure may occur when the decline from peak to minimum deviatoric stress is large. The normalisation between q_{max} and q_{min}, as used by Sadrekarimi (2014), is adopted in the present study to quantify the liquefaction susceptibility of clean sand and mixtures. The amount of reduction in undrained shear strength during liquefaction is usually characterised by the undrained brittleness index, I_B, as shown below (Bishop, 1971):

$$I_B = q_{max} - q_{min}/q_{max} \tag{6}$$

The values for I_B are in the range of 0–1, and non-flow or non-brittle behaviour (where a non-strength decline occurs during undrained static shear) is observed when $I_B = 0$. However, brittle soil behaviour or complete static liquefaction is associated with $I_B = 1$. Fig. 12 shows the undrained brittleness index for all the materials used in this study at $D_r = 10\%$ and an initial confining pressure of 100 kPa. This relative density and confining pressure were selected to investigate the effect of mixing clean sand with different percentages of fines, as clean sand samples liquefied completely at these values. Fig. 12 also indicates that the C.S sample showed liquefaction behaviour with $I_B = 1$. The I_B values of the mixtures decreased with increases in the slag content of up to 4% and then increased as the slag content increased up to 6%. This means that a slag content of more than 4% decreases the undrained shear strength of mixtures. The undrained shear strength also decreased when the sand was mixed with 3%

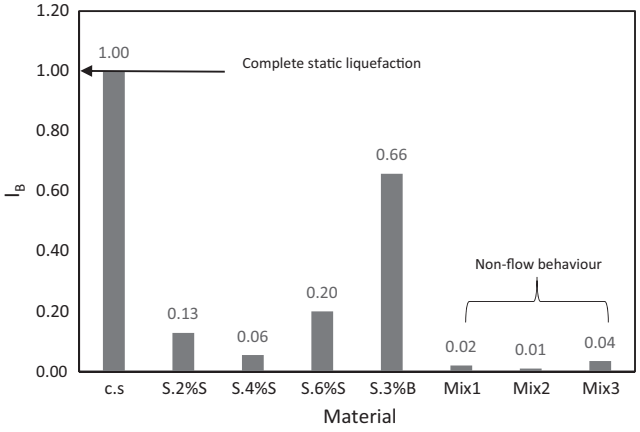

Fig. 12. Variation in I_B for all materials with $D_r = 10\%$, $B = 0.95$, and initial confining pressure of 100 kPa.

bentonite. All three mixtures – Mix 1, Mix 2, and Mix 3 – showed non-flow behaviour with very low values for I_B (near zero), and Mix 2 exhibited the lowest I_B value.

4. Conclusion

This paper presents the results of undrained static triaxial compression tests on isotropically consolidated samples of clean sand and sand mixed with various percentages of bentonite and slag. Two relative densities (10% and 20%) with three confining pressures (100, 150, and 200 kPa) were used in the experimental program. All samples were prepared by the moist tamping method. The results were analysed through the static liquefaction concept. The following conclusions can be reached:

(a) In the undrained triaxial tests under static shearing, clean Perth sand was seen to exhibit the behaviours of complete static liquefaction ($\sigma_3^- = 0$) and limited liquefaction. Very loose saturated samples with a relative density of about 10% showed complete static liquefaction under the lowest level of initial confining pressure (100 kPa). However, samples with the same relative density showed greater resistance as the confining pressure was increased. This contrasts with the usual behaviour of soils - where their resistance decreases with an increasing confining pressure. The reasons for these responses are related to the densification of the samples, as the compressibility of very loose samples increased with an increasing confining pressure and led to stable fabrics. Additionally, the excess pore pressure decreased as the confining pressure increased.

(b) Increases in the relative density of clean sand samples eventually produced a stable sand fabric. The behaviour of the samples shifted substantially from complete liquefaction to limited liquefaction due to the increased contacts between the sand particles and the decreased excess pore water pressure.

(c) Increasing the slag content up to 4% improved the shear strength of the sand–slag mixtures. The behaviour of the clean sand shifted from complete static liquefaction to non-flow behaviour with an increasing slag content. The lowest excess pore water pressures and the highest deviatoric stresses were observed with slag contents of up to 4%. Slag was seen to improve the liquefaction resistance of the sandy soil by filling the inter-particle voids and reducing the pore water pressure.

(d) The low bentonite content had an adverse impact on the behaviour of the clean sand. The pore water pressure in the sand with bentonite was higher than that in the clean sand. These effects may be due to a weakening of the soil fabric and decreases the in inter-particle contacts between particles.

(e) Mixing clean sand with two types of fines (slag and bentonite) reduced its liquefaction susceptibility. Three mixtures – Mix 1, Mix 2, and Mix 3 – showed non-flow behaviour at the three tested confining pressures. Deviatoric stresses increased with confining pressure. Mix 2 exhibited the highest deviatoric stress and the lowest excess pore water pressure.

(f) The undrained brittleness index, I_B, can be used to determine the amount of reduction in undrained shear strength during liquefaction. The I_B values ranged from 0 to 1, with non-flow behaviour observed when $I_B = 0$ and complete static liquefaction observed when $I_B = 1$.

Acknowledgements

The first author sincerely acknowledges the funding received from the Higher Committee for Education Development in the Republic of Iraq in the form of a scholarship for his PhD study. The authors recognise the use of Curtin University's Microscopy & Microanalysis Facility, whose instrumentation has been partially funded by the University, State, and Commonwealth Governments.

References

Alarcon-Guzman, A., Leonards, G., Chameau, J., 1988. Undrained monotonic and cyclic strength of sands. J. Geotech. Eng. 114, 1089–1109.

Allan, M., Kukacka, L., 1995. Blast furnace slag-modified grouts for in situ stabilization of chromium-contaminated soil. Waste Manag. 15, 193–202.

Andrade, J.E., 2009. A predictive framework for liquefaction instability. Géotechnique 59 (8), 673–682.

Australian Slag Association, 2011. Blast Furnace Slag Aggregate and Cementitious Products. Reference data sheet 1.

Been, K., Jefferies, M., 2004. Stress-dilatancy in very loose sand. Can. Geotech. J. 41, 972–989.

Belhouari, F., Bendani, K., Missoum, H., Derkaoui, M., 2015. Undrained static response of loose and medium dense silty sand of Mostaganem (Northern Algeria). Arab. J. Sci. Eng. 40, 1327–1342.

Bishop, A.W., 1971. Shear Strength Parameters for Undisturbed and Remoulded Soil Specimens. Roscoe Memorial Symposium. Cambridge University, Cambridge, Mass, pp. 3–58.
Bjerrum, L., Kringstad, S., Kummeneje, O., 1961. The Shear Strength of a Fine Sand. Norwegian Geotechnical Institute, Publication 45.
Castro, G., 1969. Liquefaction of Sand Ph.D. thesis. Harvard University, Cambridge, Massachusetts.
Dafalias, Y.F., Manzari, M., 2004. Simple plasticity sand model accounting for fabric change effects. J. Eng. Mech., ASCE 130 (6), 622–634.
Delia, N., 2010. Laboratory testing of the monotonic behaviour of partially saturated sandy soil. Earth Sci. Res. J. 14, 181–186.
El Mohtar, C., Bobet, A., Drnevich, V., Johnston, C., Santagata, M., 2013. Pore pressure generation in sand with bentonite: from small strains to liquefaction. Géotechnique 64, 108–117.
Georgiannou, V., Burland, J., Hight, D., 1990. The undrained behaviour of clayey sands in triaxial compression and extension. Geotechnique 40, 431–449.
Gratchev, I.B., Sassa, K., Osipov, V.I., Sokolov, V.N., 2006. The liquefaction of clayey soils under cyclic loading. Eng. Geo. 86 (1), 70–84.
Higgins, D., 2005. Soil Stabilisation With Ground Granulated Blast Furnace Slag. UK Cementitious Slag Makers Association (CSMA), United Kingdom.
Hird, C., Hassona, F., 1990. Some factors affecting the liquefaction and flow of saturated sands in laboratory tests. Eng. Geo. 28, 149–170.
Ibsen, L.B., 1998. The Mechanism Controlling Static Liquefaction and Cyclic Strength of Sand. Geotechnical Engineering Group, Denmark.
Ishihara, K., 1993. Liquefaction and flow failure during earthquakes. Geotechnique 43, 351–451.
Jafarian, Y., Ghorbani, A., Salamatpoor, S., Salamatpoor, S., 2013. Monotonic triaxial experiments to evaluate steady-state and liquefaction susceptibility of Babolsar sand. J. Zhejiang Uni. SCIENCE A 14, 739–750.
Konrad, J.M., 1990. Minimum undrained strength of two sand. J. Geotech. Eng. 116 (6), 932–947.
Kramer, S.L., 1996. Geotechnical Earthquake Engineering. Prentice Hall, Upper Saddle River (NJ).
Kramer, S.L., Seed, H.B., 1988. Initiation of soil liquefaction under static loading conditions. J. Geotech. Eng. 114, 412–430.
Lade, P.V., 1992. Static instability and liquefaction of loose fine sandy slopes. J. Geotech. Eng. ASCE 118 (1), 51–71.
Lade, P.V., Pradel, D., 1990. Instability and plastic flow of soils. I: Experimental observations. J. Eng. Mech. 116 (11), 2532–2550.
Leong, W., Chu, J., Teh, C., 2000. Liquefaction and instability of a granular fill material. Geotech. Test. J. 23, 178–192.
Matsuda, H., Shinozaki, H., Ishikura, R., Kitayama, N., 2008. Application of granulated blast furnace slag to the earthquake resistant earth structure as a geo-material. Proceedings of the 14th World Conference on Earthquake Engineering, Beijing, China.
Miura, S., Toki, S., 1982. Sample preparation method and its effect on static and cyclic deformation-strength properties of sand. Soils Found. 22 (1), 61–77.
Murthy, T., Loukidis, D., Carraro, J., Prezzi, M., Salgado, R., 2007. Undrained monotonic response of clean and silty sands. Géotechnique 57, 273–288.
National Research Council, 1985. Liquefaction of Soils During Earthquakes. National Academy Press, Washington, DC.
Olson, S.M., Stark, T.D., 2003. Use of laboratory data to confirm yield and liquefied strength ratio concepts. Can. Geotech. J. 40 (6), 1164–1184.
Ouf, M.E.S.A.R., 2001. Stabilisation of Clay Subgrade Soils Using Ground Granulated Blast Furnace Slag Doctoral dissertation. University of Leeds.
Park, S.S., Choi, S.G., Nam, I.H., 2014. A study on cementation of sand using blast furnace slag and extreme microorganism. J. Kor. Geotech. Soc. 30 (1), 93–101.
Pitman, T., Robertson, P., Sego, D., 1994. Influence of fines on the collapse of loose sands. Can. Geotech. J. 31, 728–739.
Poulos, S.J., Castro, G., France, J.W., 1985. Liquefaction evaluation procedure. J. Geotech. Eng. 111 (6), 772–792.
Pradel, D., Lade, P.V., 1990. Instability and plastic flow of soils. II: Analytical investigation. J. Eng. Mech. 116 (1), 2551–2566.
Rabbani, P., Daghigh, Y., Atrechian, M.R., Karimi, M., Tolooiyan, A., 2012. The potential of lime and grand granulated blast furnace slag (GGBFS) mixture for stabilisation of desert silty sands. J. Civ. Eng. Res. 2 (6), 108–119.
Rahman, M.M., Lo, S., 2014. Undrained behaviour of sand-fines mixtures and their state parameter. J. Geotech. Geoenviron. 140, 04014036-1–04014036-12.
Riemer, M.F., Seed, R.B., Nicholson, P.G., Jong, H.L., 1990. Steady state testing of loose sands: limiting minimum density. J. Geotech. Eng. 116, 332–337.
Sadrekarimi, A., 2014. Static liquefaction-triggering analysis considering soil dilatancy. Soils Found. 54 (5), 955–966.
Schofield, A., Wroth, P., 1968. Critical State Soil Mechanics. McGraw-Hill, London.
Seed, H.B., Idriss, I.M., Arango, I., 1983. Evaluation of liquefaction potential using field performance data. J. Geotech. Eng. 109, 458–482.
Sladen, J.A., D'Hhollander, R.D., Krahn, J., 1985. The liquefaction of sands, a collapse surface approach. Can. Geotech. J. 22 (4), 564–578.
Tang, X.W., Ma, L., Dieudonné, S., 2013a. Influence of bentonite content on the static liquefaction behaviour of sand. In: Advanced Materials Research, vol. 684. Trans Tech Publications, pp. 154–158.
Tang, X.W., Ma, L., Shao, Q., 2013b. Experimental investigation on effect of bentonite content to the liquefaction potential in saturated sand. J. Geotech. Eng. 18, 1409–1417.
Thevanayagam, S., Shenthan, T., Mohamn, S., Liang, J., 2002. Undrained fragility of clean sands, silty sands, and sandy silts. J. Geotech. Geoenviron. 128, 849–859.
Vaid, Y., Chern, J., 1985. Cyclic and monotonic undrained response of saturated sands. Advances in the Art of Testing Soils Under Cyclic Conditions, ASCE, 120–147.
Vaid, Y.P., Sivathayalan, S., 2000. Fundamental factors affecting liquefaction susceptibility of sands. Can. Geotech. J. 37 (3), 592–606.
Veith, G., 2000. Essay competition – green, ground and great: soil stabilization with slag. Build. Res. Inf. 28, 70–72.
Verdugo, R., Ishihara, K., 1996. The steady state of sandy soils. Soil Found. 36 (2), 81–91.
Wei, L., Yang, J., 2014. On the role of grain shape in static liquefaction of sand–fines mixtures. Géotechnique 64, 740–745.
Yamamuro, J.A., Covert, K.M., 2001. Monotonic and cyclic liquefaction of very loose sands with high silt content. J. Geotech. Geoenviron. 127, 314–324.
Yamamuro, J.A., Lade, P.V., 1997. Static liquefaction of very loose sands. Can. Geotech. J. 34, 905–917.
Yamamuro, J.A., Lade, P.V., 1998. Steady-state concepts and static liquefaction of silty sands. J. Geotech. Geoenviron. 124 (9), 868–877.
Yamamuro, J.A., Wood, F.M., Lade, P.V., 2008. Effect of depositional method on the microstructure of silty sand. Can. Geotech. J. 45, 1538–1555.
Yand, J., Wei, L., 2012. Collapse of loose sand with the addition of fines: the role of particle shape. Geotechnique 62, 1111–1125.
Yand, S., Lacasse, S., Sandven, R., 2006. Determination of the transitional fines content of mixtures of sand and non-plastic fines. Geotech. Test. J. 29, 1–6.
Yi, Y., Liska, M., Al-Tabbaa, A., 2013. Properties of two model soils stabilized with different blends and contents of GGBS, MgO, lime, and PC. J. Mater. Civ. Eng. 26, 267–274.
Yoshimine, M., Robertson, P.K., Wride, C.E., 1999. Undrained shear strength of clean sands to trigger flow liquefaction. Can. Geotech. J. 36, 891–906.